



1 **Dispersal dynamics along river corridors modulate impact of**
2 **climate change on treeline shift in Hengduan Mountain**

3
4 Linfeng Wei^{1,2}, Jian Ni³, Xianyong Cao⁴, Stefan Kruse¹

5
6 ¹ Alfred Wegener Institute, Helmholtz Centre for Polar and Marine Research, Potsdam, Germany

7 ² Institute of Biochemistry and Biology, University of Potsdam, Potsdam, Germany

8 ³ College of Life Sciences, Zhejiang Normal University, Jinhua, China

9 ⁴ Alpine Paleocology and Human Adaptation Group (ALPHA Group), State Key Laboratory of Tibetan Plateau
10 Earth System, Environment and Resources, Institute of Tibetan Plateau Research, Chinese Academy of Sciences,
11 Beijing, China

12
13 **Correspondence:** Linfeng Wei (linfeng.wei@awi.de) and Stefan Kruse (stefan.kruse@awi.de)

14
15 **Abstract**

16 Alpine treelines are expected to respond to climate warming, but the magnitude and direction of treeline shifts
17 often vary across mountain landscapes. In the Hengduan Mountains, river corridors may shape how forest
18 expansion is expressed as lateral and elevational treeline shifts, with important implications for future alpine
19 habitat loss. Here, we modified and applied the spatially explicit individual based model LAVESI to simulate
20 treeline dynamics along four major river corridors: the Dadu, Lancang, Nu, and Yalong rivers. Simulations
21 covered the historical period from 1940 to 2020 and the future period from 2020 to 2100 under SSP1-2.6, SSP2-
22 4.5, and SSP5-8.5.

23
24 During the historical period, simulated treeline shifts were gradual but river specific. Lateral changes were
25 strongest in the Lancang and Nu rivers, intermediate in the Yalong River, and weak in the Dadu River. Elevational
26 changes were more limited, with the Lancang River showing the clearest upward shift and the Nu River remaining
27 close to stable. After 2020, lateral treeline shifts became stronger and more divergent among river corridors and
28 scenarios. In most rivers, future lateral advance increased, with SSP2-4.5 generally producing relatively high
29 cumulative expansion. Elevational shifts followed a related but not identical pattern: the Lancang River
30 maintained the strongest upward trend, the Dadu and Yalong rivers showed moderate increases, and the Nu River
31 remained weakly responsive. The relationship between lateral and elevational changes therefore varied among
32 rivers, indicating that horizontal boundary reorganization did not always translate into comparable upslope shift.

33
34 Treeline invasion potential was also uneven. The Dadu River frequently reached the predefined upper limit,
35 although this result should be interpreted in relation to the shorter simulation extent. In contrast, most simulations
36 for the Lancang, Nu, and Yalong rivers remained below the upper limit by 2100, suggesting incomplete occupation
37 of the available treeline tundra ecotone. Overall, our results indicate that future treeline shifts in the Hengduan
38 Mountains are likely to remain spatially heterogeneous across river corridors, with different implications for alpine
39 habitat vulnerability. This vulnerability should therefore be evaluated at the river corridor scale, where lateral
40 expansion, elevational advance, and local topographic and ecological settings jointly shape the potential for future
41 forest expansion.

42 **1 Introduction**

43 **1.1 Alpine treeline dynamics in the Tibetan Plateau**

44 Alpine treeline is primarily constrained by climate and its upward shifts have been widely observed by the increase
45 of growing season temperature (Körner, 2021; Sigdel et al., 2024). Nevertheless, evidence also suggests that the
46 treeline responses to climate are varied and often lag behind climate change due to regional differences and from



47 diverse ecosystem compositions such as acting on seed dispersal limitations (Harsch et al., 2009; Holtmeier &
48 Broll, 2005; Kruse et al., 2019; Kruse & Herzschuh, 2022). Where treeline does advance, forest expansion can
49 replace alpine ecosystems and compress high-elevation habitats that are inherently limited in area, with potentially
50 severe consequences for alpine biodiversity (Pauli et al., 2012; Dirnböck et al., 2011; Wang et al., 2022). These
51 dynamics highlight the need to focus on climate-sensitive mountain regions to better understand and predict
52 treeline dynamics under ongoing environmental change.

53

54 Alpine treeline patterns on the Tibetan Plateau are highly heterogeneous, reflecting pronounced spatial variation
55 in climate, topography, and ecosystem structure (Chen et al., 2015; Piao et al., 2019). Modern ecological and
56 remote-sensing studies show that treeline responses to recent warming vary across the Tibetan Plateau, and not
57 all treelines have observed upshift (e.g., Wang et al., 2019; Zou et al., 2022; Peng et al., 2024). Palaeoecological
58 studies further indicate that treeline positions on the Tibetan Plateau and its southeastern margin have shifted
59 repeatedly during the Holocene in response to climatic fluctuations, with additional human influence in some
60 areas (e.g., Kramer et al., 2010; Liu et al., 2021; Xu et al., 2025). Hengduan Mountain area, located at the east and
61 south border of Tibetan Plateau, is the worldwide biodiversity hotspot with a rich endemic alpine flora (Ding et
62 al., 2020). This area formed a highly heterogeneous environment and completed alpine altitudinal zonation under
63 the combined effect of monsoon and orogenic uplifts, which plays a key role in species diversification, persistence
64 and dispersal (Li et al., 2014; Antonelli et al., 2018). The widespread alpine treeline area, also known as the high
65 mountain ecotone, is sensitive to climate change and other environmental variables (Di Musciano et al., 2020;
66 Weckworth et al., 2013; Vintsek et al., 2022). Therefore, understanding the driving mechanism of treeline shift
67 and how it is corresponding to climate change is essential for revealing the alpine ecosystem and predicting future
68 changes of endemic species.

69

70 **1.2 River corridors as dispersal pathways across alpine ecotones**

71 Forest expansion beyond the upper treeline has increasingly led to the replacement of alpine shrublands and
72 meadows, thereby reshaping the structure and functioning of high elevation ecosystems (Wang et al., 2022; Sigdel
73 et al., 2024). The extent and rate of forest alpine replacement vary markedly across regions and are influenced by
74 differences in snow regime, moisture availability, nutrient limitation, and biotic interactions, which can produce
75 delayed, uneven, or locally suppressed treeline advance (Rees et al., 2020; Gustafson et al., 2021; Zheng et al.,
76 2024). Part of this variation may also reflect broader landscape structure. Treeline ecotones are increasingly
77 understood as spatially heterogeneous systems in which topography, treeline form, and local environmental
78 context jointly influence where upward movement occurs and where it remains constrained (Holtmeier and Broll,
79 2005; Bader et al., 2021; Treml and Chuman., 2015).

80

81 Within this landscape framework, river systems may provide an important mechanism through which forest
82 expansion beyond the upper treeline becomes spatially organized. At broad spatial scales, river networks are
83 increasingly recognized as ecological corridors that shape dispersal, connectivity, and biodiversity patterns across
84 landscapes (Rinaldo et al., 2018). For plants, river corridors can influence vegetation composition and
85 regeneration by facilitating water-mediated dispersal, maintaining connected riparian habitats, and generating
86 dynamic microsites through flooding, sediment deposition, erosion, and disturbance (Nilsson et al., 2010;



87 Corenblit et al., 2007; Gurnell et al., 2016). In this sense, rivers are not merely passive topographic features but
88 active ecological interfaces between terrestrial and aquatic systems, with important consequences for vegetation
89 structure, ecosystem functioning, and landscape connectivity (Naiman and Décamps, 1997; Riis et al., 2020; Wohl
90 et al., 2017).

91

92 For alpine ecotones, river valleys and riparian zones may therefore act both as dispersal pathways and as
93 environmental filters. Connected valley habitats and buffered microclimates may increase opportunities for seed
94 arrival, seedling establishment, and upslope movement, whereas exposed ridges and fragmented terrain may
95 restrict movement and contribute to uneven treeline advance (Rupp et al., 2001; Wei et al., 2013; Holešťová and
96 Douda, 2022; Zhang et al., 2023). However, connectivity alone is unlikely to determine whether forest migration
97 is realized. The establishment and survival of trees beyond the current treeline also depend on topoclimatic
98 buffering, microsite conditions, disturbance regimes, and distance to seed sources (Greenwood et al., 2015; Vitali
99 et al., 2017; Rita et al., 2023; Hamid et al., 2023). The Hengduan Mountains provide a particularly suitable setting
100 for examining these processes, because major north–south river systems, including the Jinsha, Lancang, and Nu
101 rivers, have carved deeply incised parallel valleys through high mountain ranges, producing sharp elevational
102 gradients and strong habitat heterogeneity within short distances (Sherman et al., 2008; Zhang et al., 2021).

103 **1.3 Individual-based models can capture nonlinear treeline responses**

104 Treeline dynamics have been investigated using several modelling frameworks. Empirical statistical models,
105 including generalized linear models and partial least squares regression, have been widely used to identify broad
106 climatic controls on treeline position and change. For example, generalized linear models have been applied to
107 model the potential distribution of the Himalayan treeline species *Betula utilis*, whereas partial least squares
108 regression has been used to analyse large scale treeline dynamics in the Hengduan Mountains (Bobrowski et al.,
109 2017; Tian et al., 2022). More flexible statistical approaches, particularly generalized additive models, are useful
110 for capturing nonlinear responses and environmental thresholds. These approaches have been used to analyse
111 mortality and growth responses at alpine treelines and to assess the relative roles of climate and herbivory in
112 treeline dynamics (Barbeito et al., 2012; Mienna et al., 2020). In parallel, machine learning approaches and species
113 distribution models have become increasingly common because they can characterize complex environmental
114 relationships and estimate potential distribution changes under future climates. For instance, support vector
115 machines and XGBoost have been used to analyse deviations between actual and thermal treelines on Yulong
116 Snow Mountain, while MaxEnt based studies have been widely applied in the Himalaya to estimate climatic
117 suitability for treeline forming species (Lin et al., 2024; Bobrowski et al., 2021). However, because these
118 approaches are primarily correlative, they are less well suited to representing the demographic processes that
119 ultimately govern treeline advance, stability, or retreat.

120 In this context, individual based process models provide a useful complement to correlative approaches because
121 they can explicitly represent demographic processes such as growth, seed production, dispersal, establishment,
122 and mortality. This makes them better suited to examining transient dynamics, migration lags, and delayed stand
123 responses that are difficult to infer from statistical relationships alone. LAVESI is one such spatially explicit
124 model and has been applied mainly to larch dominated treeline systems to investigate how demographic
125 constraints influence treeline advance, stability, and retreat (Kruse et al., 2016). Subsequent developments



126 improved the representation of dispersal and migration and incorporated additional processes including permafrost
127 vegetation interactions and adaptive responses, thereby broadening its potential application under heterogeneous
128 environmental conditions (Kruse et al., 2018; Kruse et al., 2022; Gloy et al., 2023). In the Hengduan Mountains,
129 modelling studies relevant to forests and treelines have so far been dominated by remote sensing, spatial statistics,
130 machine learning, and species distribution models, while process based individual or gap models remain scarce.
131 Remote sensing studies have documented both treeline position shifts and structural densification (Tian et al.,
132 2022; Zou et al., 2022), machine learning has been applied to identify actual treelines and their climatic deviations
133 (Lin et al., 2024), and MaxEnt based studies have been used to project alpine vegetation or tree species suitability
134 under future climates (He et al., 2020; Li et al., 2020). By contrast, process based demographic modelling has so
135 far played a relatively limited role in treeline studies from the Hengduan Mountains, although related gap
136 modelling has been explored in nearby mountain systems, such as a FAREAST application on Gongga Mountain
137 (Huo et al., 2010). In this context, LAVESI provides a useful framework not simply because it has not yet been
138 widely applied in this region, but because its explicit representation of growth, dispersal, establishment, and
139 mortality is well suited to analysing the spatially heterogeneous and potentially lagged treeline dynamics observed
140 here.

141 **Research Objective**

142 Our overarching aim is to understand forest upslope migration and assess how the topography of river corridors
143 influences this process, in order to estimate future rates. Specifically, we address three research questions by
144 developing a new version of LAVESI to simulate forest dynamics along river corridors with contrasting
145 topographic settings in the Hengduan Mountains, driven by climate trajectories from before the Holocene
146 climatic optimum through to multiple future climate change scenarios:

- 147 1. To what extent, and over what time scales, will treelines shift in response to historical and
148 contemporary climate change and associated ecological processes along mountain river corridors?
- 149 2. How do contrasting river systems mediate treeline migration over the coming decades under different
150 climate change scenarios?
- 151 3. Do river corridors constitute climate-sensitive hotspots of future treeline advance and associated alpine
152 habitat loss in the Hengduan Mountains?

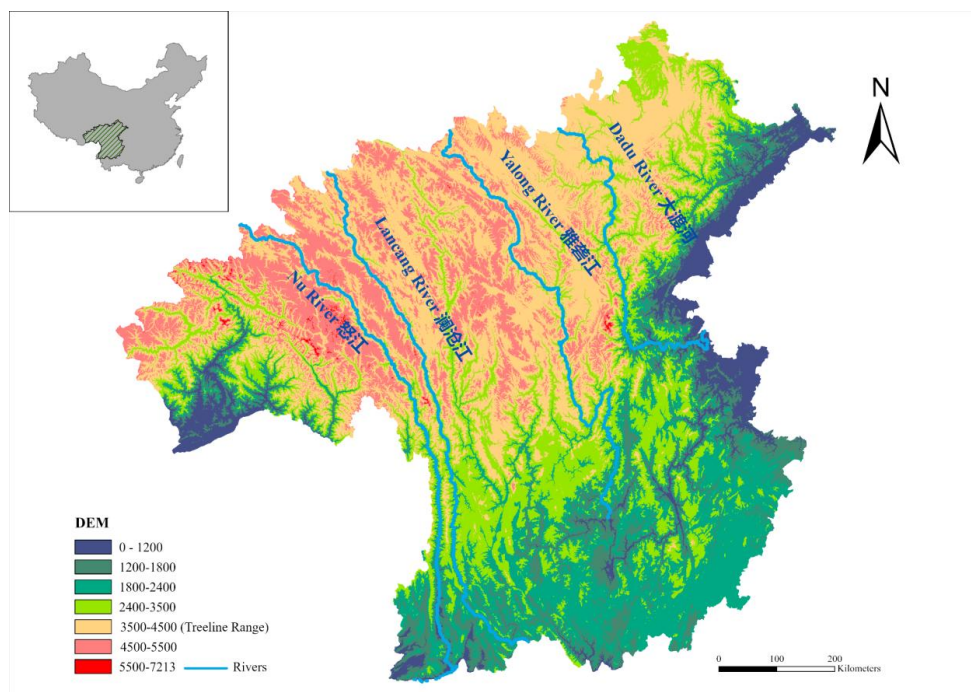
153 **2 Materials and Methods**

154 **2.1 Study system Hengduan mountains**

155 Located at the southeastern margin of the Tibetan Plateau, the Hengduan Mountains form the longest and widest
156 typical north–south-oriented parallel mountain system in China. Long-term tectonic uplift associated with the
157 Indian-Eurasian collision, together with intense river incision, has produced a highly dissected landscape
158 characterized by closely spaced high mountains and deeply incised valleys (Integrated Scientific Expedition to
159 Qinghai-Tibet Plateau, Chinese Academy of Sciences, 1997; Xing and Ree, 2017). This strong topographic relief
160 creates pronounced elevational and climatic gradients, ranging from warm, low-elevation valleys to cold subalpine
161 and alpine zones above the treeline (Fig. 1). The major river systems, including the Nu, Lancang, Yalong, and



162 Dadu rivers, are embedded within the north-south-oriented mountain valley terrain and connect headwater areas
163 with downstream valleys across pronounced elevational, climatic, and vegetation gradients. These features make
164 the Hengduan Mountains an ideal region for examining spatial variation in alpine treeline patterns across complex
165 mountain-river systems.



166

167 **Figure 1.** Digital elevation model of the study area showing elevation zones, the treeline range, and major river systems. The
168 inset map in the upper left shows the location of the study area within mainland China.

169 2.2 The LAVESI model and setup

170 2.2.1 Model description

171 In this study, we used the individual-based, spatially explicit model LAVESI (Large Vegetation Simulator, Fig.
172 2) (Kruse et al., 2016), which was originally developed for *Larix gmelinii* in northeastern Siberia and simulates
173 the full life cycle of larch species. Each simulation step represents one year and includes a series of ecological
174 processes implemented sequentially as submodules. At the start of each annual cycle, an environmental update is
175 conducted. Monthly mean temperature, monthly precipitation sums, and a weather index are used to derive daily
176 environmental conditions, while competition is assessed using an annually updated map of tree population density.
177 The model then simulates seed production, seed dispersal, seedling establishment, and competition-dependent tree
178 growth, followed by ageing and mortality. LAVESI already incorporates many of the key factors affecting treeline
179 migration and has been further extended to include wind-related seed dispersal (Kruse et al., 2018), landscape
180 topography and additional boreal tree species (Kruse et al., 2022).

181 The detailed model processes and equations summarized in this section follow the original LAVESI model



182 descriptions by Kruse et al. (2016, 2019). They are presented here to clarify the model implementation used in
183 this study, while the species parameterization and simulation settings were adapted for the Hengduan Mountain.

184

185 *Initialisation:* The environmental information (elevation, slope, terrain water index) of the simulated area is read
186 in and filled in the model's structures. The weather provided in monthly temperature and precipitation values is
187 read for a given number of years. Each simulation run starts with an empty area and seeds are introduced to the
188 area during a spin-up period at the start of the model.

189

190 *Environment:* As density map is calculated for the area in which the density influence is recorded for the trees.
191 The competition between trees is calculated based on the basal diameter in a given area of the density map (Eq.
192 (1)). The active-layer depth is estimated based on the number of days exceeding 0°C.

$$\text{density influence}(x_coord, y_coord) = \frac{\text{diameter}_{\text{basal}}}{\sqrt{x_{\text{coord}}^2 + y_{\text{coord}}^2 + 1}} \quad (1)$$

193

194 *Growth:* The maximal growth is calculated based on an average of ten years' climate data. The basal growth (Eq.
195 (2)) of one individual for the year is then derived from this by including the density index of the tree. Based on
196 the diameter, the tree height is estimated (Eq. (3)).

$$\text{Growth}_{\text{max,diameter}} = \left(\text{precipitation} * \text{Growth}_{\text{standard,diameter}} * \right. \\ \left. \left(\frac{1}{f_{\text{AATNDD}}} * \text{AATI} + \left(1 - \frac{1}{f_{\text{AATNDD}}} \right) * \text{net degree days} \right) \right) * (1 - \text{TDEI}) \quad (2)$$

197

$$\text{height} = \begin{cases} 44.43163 * \text{diameter}_{\text{basal}}, & \text{height} < 1.3 \text{ m} \\ (7.02 * \sqrt{\text{diameter}_{\text{breast}}})^2 + 130, & \text{height} \geq 1.3 \text{ m} \end{cases} \quad (3)$$

198

199

200 *Seed dispersal:* Seeds that are still within cones are dispersed, the direction and distance are randomly determined
201 influenced by wind data (Eq. (4)). When seeds leave the extent of the transect to either the east or west, they are
202 reintroduced from the opposite site, to simulate a larger forest and avoid the loss of many seeds.

$$\text{distance} = \text{sqrt} \left(2 \left(\text{release height} * \text{wind} \frac{\text{speed}}{\text{fall}} \text{speed} \right)^2 * (-\log(\text{rand})) + \frac{1}{2} \text{distance ratio} * \right. \\ \left. \text{rand}^{-1.5} \right) \quad (4)$$

203

204 *Seed production:* Once a tree has reached the height of maturation, based on a pre-generated distribution randomly
205 assigned, it produces seeds. The amount produced in each year is based on the height of the tree, competition, and
206 the weather (Eq. (5)).

$$\text{seeds produced} = [\text{factor}_s * \text{Diameter}_{\text{basal}} * (1.0 - (\text{height}/(50 \text{ m}))^{-1.0})] \quad (5)$$

207

208 *Establishment:* Seeds that are on the ground germinate based on weather conditions (Eq. (6)).

$$\text{probability to germinate}(\text{year}) = \text{background germination rate} + \quad (6)$$



$$\left(\text{weather quality factor} * \frac{\text{Growth}_{(\text{max,basal})(\text{year})}}{\text{Growth}_{\text{standard,basal}}} \right)$$

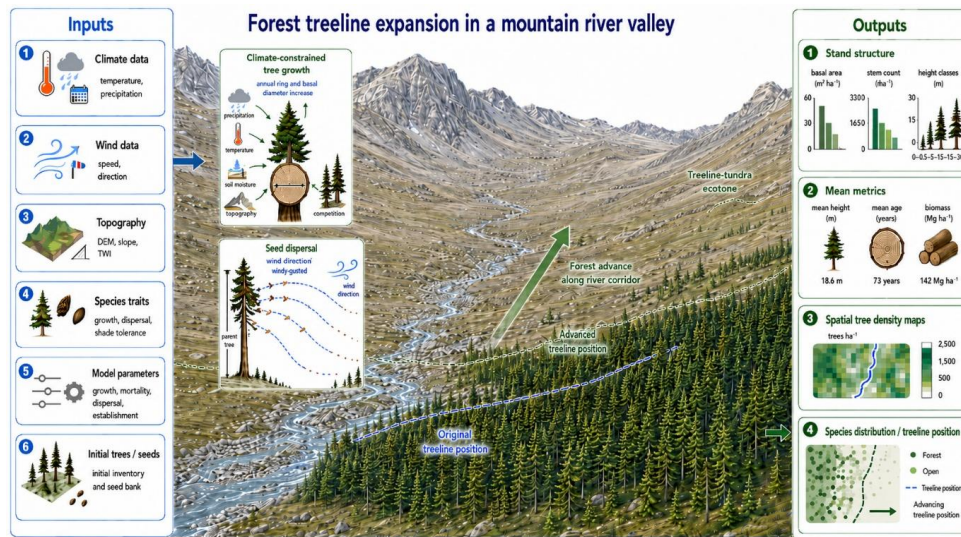
209

210 *Mortality*: The probability of death is calculated for each tree and, based on that, it is semi-randomly determined
 211 whether the tree dies and is removed from the simulation. The calculation is based on long-term weather values,
 212 the calculated drought strength, competition of surrounding trees, the age and size of the tree, and a base mortality
 213 rate. For each of these a mortality value is calculated, these are then summed up and compared to a randomly
 214 generated number. If the sum of death probabilities is larger the tree dies. The death of seeds is determined at this
 215 step as well, although the mortality rate for these is fixed.

216

217 *Ageing*: The last step is an increase in the age of both the seeds and the trees. Since every year is simulated, the
 218 age is advanced by once each cycle. The seeds are removed once they have reached a certain (3 years) age limit.
 219

220



221

221 **Figure 2.** Conceptual framework of simulated forest treeline expansion in a mountain river valley. (This figure
 222 was created with the assistance of an AI-based image generation tool and subsequently reviewed and edited by
 223 the authors to ensure conceptual accuracy.)

224 **2.2.2 Hengduan species parameter set**

225 The initial version of LAVESI focused on genus *Larix* (Kruse et al. 2016). This conifer species forms the treeline
 226 in Eurasian arctic treelines. Therefore, we decided to extend the range of application especially to include
 227 Hengduan Mountain treeline forming species by selecting species based on local floristic records. We summarized
 228 species lists from the Flora Xizangica (Integrated Scientific 195 Expedition to Qinghai-Tibet Plateau, Chinese
 229 Academy of Sciences, 1983–1987), the Flora of Sichuan (Gao et al., 1981), and the Flora of Yunnan (Kunming
 230 Institute of Botany, Chinese Academy of Science, 1977-2006), and identified the shared gymnosperm species
 231 among these regions, yielding a total of 50 species. For the necessary parameters, we collected them from trait



232 datasets, handbook, Flora and expert experiences (Table S1).

233

234 Based on field surveys conducted in the Hengduan Mountains in 2023 and 2024, we collected measurements of
235 individual trees from plot records along the selected river system area, including tree height and stem diameter.

236 To describe the relationship between tree height and stem size, we built height–diameter models for each target
237 species. We first selected records for the target species and removed observations with missing or zero values for
238 height or diameter. Tree height was converted to cm, and diameter was converted to mm. Depending on the dataset
239 (Jin et al., 2026), diameter was represented by diameter at breast height (DBH) or basal diameter.

240 Because the relationship between height and diameter was nonlinear, both variables were transformed using the
241 natural logarithm before model fitting. We then fitted a logistic nonlinear model in log space:

$$\ln(H) = \frac{A}{1 + \exp\left(\frac{x_m - \ln(D)}{s}\right)} \quad (7)$$

242 where H is tree height, D is DBH or basal diameter, A is the upper asymptote, x_m is the midpoint parameter, and
243 s is the scale parameter (Eq. (7)).

244 Initial parameter values were obtained with a self-starting Logistic function. Final parameter estimates were then
245 fitted using generalized nonlinear least squares (GNLS) with function “gnls” from R-package “nlme” (Pinheiro et
246 al. 2026). The fitted model was used in LAVESI to estimate tree height for the observed and simulated diameter
247 range and to draw height–diameter curves for each species.

248 We collected tree ring data from published datasets archived in the International Tree Ring Data Bank (ITRDB)
249 (Grissino-Mayer and Fritts, 1997). The data were accessed through the NOAA World Data Service for
250 Paleoclimatology. We restricted the search to sites within China and then queried the database using the Latin
251 names of the target conifer species. Finally, we found 10958 individual ring-width series for 21 species (Table S2).

252 Radial growth was modelled as an exponential quadratic function of stem size:

$$G(D) = \exp(a + b \cdot D + c \cdot D^2) \quad (8)$$

253 where $G(D)$ is the annual radial increment at stem size D , a is the intercept (gdbasalconst), b is the linear size
254 effect (gdbasalfac), and c is the quadratic size effect (gdbasalfacq) (Eq. (8)). The quadratic term allows growth to
255 increase at small sizes and decline again at larger sizes, thus representing a unimodal growth trajectory.

256 2.2.3 River transect simulation setup

257 We selected four representative river transects in the Hengduan Mountains, as major rivers in this region are
258 predominantly oriented along a north–south axis and traverse a large proportion of the landscape. Acting as key



259 ecological corridors, they play a crucial role in maintaining ecosystem stability and facilitating species migration.
260 Based on the Tibetan treeline range defined by Xu (2025), we determined the longitudinal extent of the simulation
261 area for each river according to its elevational range (Table 1). Xu *et al.* suggested that the regional treeline occurs
262 approximately between 3500 and 4500 m. Therefore, for each river, we defined the lower-elevation section
263 extending from the downstream starting point to the upper limit of this treeline range as the spin-up and seed
264 introduction zone (Fig. A1). This zone allowed the model to establish a stable initial vegetation state and seed
265 availability before entering the target treeline-tundra ecotone. The remaining upstream section, generally located
266 above the treeline range, was then treated as the treeline-tundra ecotone simulation zone. We then applied a 30 m
267 buffer on both sides of the river centreline, which defined the width of the simulation area. In addition, a spin up
268 and seed introduction zone was included before the treeline-tundra ecotone to allow the simulated forest to
269 establish under continuous seed input and approach a near stable state. The extent of this zone was defined
270 according to the spatial range in which most simulated species were concentrated in the model output. All spatial
271 operations were carried out in ArcGIS Pro.

272
273

Table 1. Basic information for selected river transects.

River	Full Length in Simulation(m)	Spin-up and Seed Introduction Length(m)	Treeline-tundra Ecotone Length(m)
Dadu 大渡河	26625	5000	21625
Lancang 澜沧江	252355	200000	52355
Nu 怒江	339730	290000	49730
Yalong 雅砻江	308035	280000	28035

274 2.3 Forcing data

275 2.3.1 Past and historical climate data

276 LAVESI requires monthly mean temperature, monthly mean precipitation data, and 6-hourly wind speed and
277 direction as input data. Temperature, precipitation and wind data were derived from the transient MPI
278 ESM_Glac1d-P3 data (Max Planck Institute for Meteorology Earth System Model, 1.875° resolution) (Kapsch *et al.*, 2022). Past temperature and precipitation data was downscaled and bias corrected to monthly values using the
279 CRU TS data (years 1901-present, 0.5° resolution) which was derived by interpolating weather station
280 observations (Harris *et al.*, 2020). Wind speed and direction was downscaled to four daily values using the
281 Copernicus ERA5 (European ReAnalysis) dataset and adding monthly variation patterns. This global dataset (0.25°
282 resolution) covers data from 1940 to present at 10 m height (Hersbach *et al.*, 2020). Specially, to the wind data in
283 future phase from 2021-2100, we performed random sampling based on the high resolution data from 1940 to
284 2020 in order to reduce the influence of the lower data resolution in the future phase.

285
286

287 2.4.2 Future climate data

288 Future temperature, precipitation and wind data were derived from MPI-ESM 1.2 LR (Max Planck Institute for
289 Meteorology Earth System Model version 1.2 low resolution, 1.875°). This data was generated for the Coupled



290 Model Intercomparison Project Phase 6 (CMIP 6) (Wieners et al., 2019). To represent future climate forcing, three
291 Shared Socioeconomic Pathway scenarios were used, namely SSP1-2.6, SSP2-4.5, and SSP5-8.5. These scenarios
292 span a range from relatively low to high future radiative forcing and are widely used to assess climate related
293 ecological responses under contrasting future conditions (Meinshausen et al., 2020).

294

295 2.3.3 Environment

296 To apply LAVESI to the study areas of this thesis, environmental variables including elevation, slope, and surface
297 moisture were derived from a 30 m resolution digital elevation model (Ho et al., 2025). The digital elevation
298 model was used to calculate slope and the Topographic Wetness Index (TWI), while water bodies were excluded
299 through masking. These spatial processing steps were carried out in ArcGIS Pro to generate ready to use input
300 files for LAVESI. The buffered river shapefiles were used as masks, from which the corresponding elevation,
301 slope, and TWI were extracted. The data package will be made publicly available at final publication on Zenodo.

302

303 2.3.4 Model adjustments

304 The local version extends LAVESI-WIND specifically for treeline simulations in the Hengduan Mountains and
305 river transects. On the input side, it no longer relies only on fixed DEM, slope, and TWI files as in the official
306 version; instead, it uses “weatherchoice” codes to identify river transects such as the Dadu, Lancang, Nu, and
307 Yalong rivers, and automatically reads the corresponding treeline environmental inputs, including DEM, slope,
308 and TWI, together with specific Hengduan climate and wind data. On the output side, it adds customized treeline
309 outputs, such as “maxposition”, which records, by species, the maximum position reached by individuals taller
310 than 1.3 m, allowing direct tracking of treeline advance. It also produces simplified datatrees files at selected years,
311 retaining key variables such as Y-position, species, and tree height, which can be used for further analysis in
312 summary treeline tables.

313

314 2.4 Simulation tests

315 2.4.1 Parameters setting

316 All simulations were forced with the same parameter settings and climate input structure. The difference among
317 the four river simulations was the topographical setting of the river corridors, which determined the spatial
318 configuration of the simulation area and the associated environmental context. Therefore, differences in simulated
319 treeline dynamics can be interpreted primarily in relation to the different corridor settings rather than to changes
320 in model parameterization. The relevant parameters that were used for all simulations are listed in Table 2.

321 **Table 2.** Important parameters setting.

Parameter	Value	Description
elevationoffset	900	Tuning variable for adjusting the baseline height of the topography.
weatherchoice	1000X00404	Setting for the different scenarios and



		rivers. X here represents different river selections.
lastyearweatherdata	25151	Determined by the available input data series (final year + 1), setting of year 25151 allows the final simulation year to be 2100 CE
simduration	15150	Duration of the simulation period, shorter than lastyearweatherdata means starting later in time
seedintro	1	Binary switch to enable seed input to the simulated area
yearswithseedintro	1000	Years of seed introduction at the beginning of each simulation
seedintronumber	510	Number of seeds introduced per ha per year (for eachyearswithseedintro)
seedintropermanent	1	Binary switch to enable introduction of a low number of seeds into the simulation area as background seed rain
seedintronumberpermanent	51	The number of seeds introduced per ha per year and plot if switched on
seedwinddispersalmode	2	Setting to determine the positions for introduced seeds that is randomly into the simulated area in our case
seedintro_maxy	5000	The setting of the maximum position of introduced seeds in m, starting at the lowest points of the river corridor

322

323 **2.4.2 Calibration based on plot datasets**

324 To identify the most suitable climatic setting for the simulations, we calibrated the parameter weatherchoice,
 325 which represents different combinations of climate input data, using all available plot data (plots 401–472). For
 326 each plot, local climate and topographic information were first extracted from its spatial location and used as
 327 model input. We then ran simulations under a range of elevation offset values. The elevation offset is a tuning
 328 parameter that adjusts the climatic conditions represented in the simulation area instead of directly applying a
 329 uniform lapse rate allowing fine tuning especially in topographically complex topographies where the local
 330 climate differs likely from the mean that is provided by the data sources as a mean value over a larger area. Model
 331 performance was evaluated by comparing simulated outputs with field observations in two steps. First, we
 332 assessed whether the simulated community type matched the observed plot type, that is, whether the plot was
 333 represented as forest, shrubland, or meadow. Second, we compared the maximum height of the three tallest
 334 observed trees in each plot with the height of the tallest simulated tree individual. The observed and simulated
 335 results were visualized and compared using ggplot2 (Wickham, 2016), and plot 404 showed the best overall
 336 agreement between field observations and simulation output. It was therefore selected as the reference plot for
 337 further calibration. Based on this plot, the elevation offset was varied from –1000 m to +1000 m in increments of
 338 100 m in order to determine which setting most closely reproduced the observed composition and structure of the



339 real treeline ecotone.

340 2.4.3 Simulation of treeline expansion

341 To reduce stochastic effects, each river corridor was simulated with 100 replicate runs on the high performance
342 computing platform. Each run covered 15,150 model years and extended to the year 2100 CE. The initial time
343 phase acted as the spin-up phase, and we analysed only the final 160 years of each simulation, corresponding to
344 1940–2100 CE.

345 For each year and species, the model output recorded the maximum simulated position. Lateral (upslope, along
346 the river corridor) treeline position was then derived from these annual outputs using a rule-based definition. We
347 first selected species with more than 1000 individuals, then scanned the spatial distribution using a 100 m moving
348 window. A window was considered valid when it contained at least 100 individuals, and a treeline was accepted
349 only if such valid windows formed a continuous segment of at least 100 m. The uppermost position satisfying
350 these criteria was defined as the annual lateral treeline.

351 Elevational treeline position was derived by mapping the simulated lateral treeline positions onto the digital
352 elevation model using R-version 4.3.3 (R core team,2023). For each annual treeline position, the corresponding
353 elevation value was extracted from the 30 m DEM, allowing us to reconstruct yearly changes in treeline elevation.

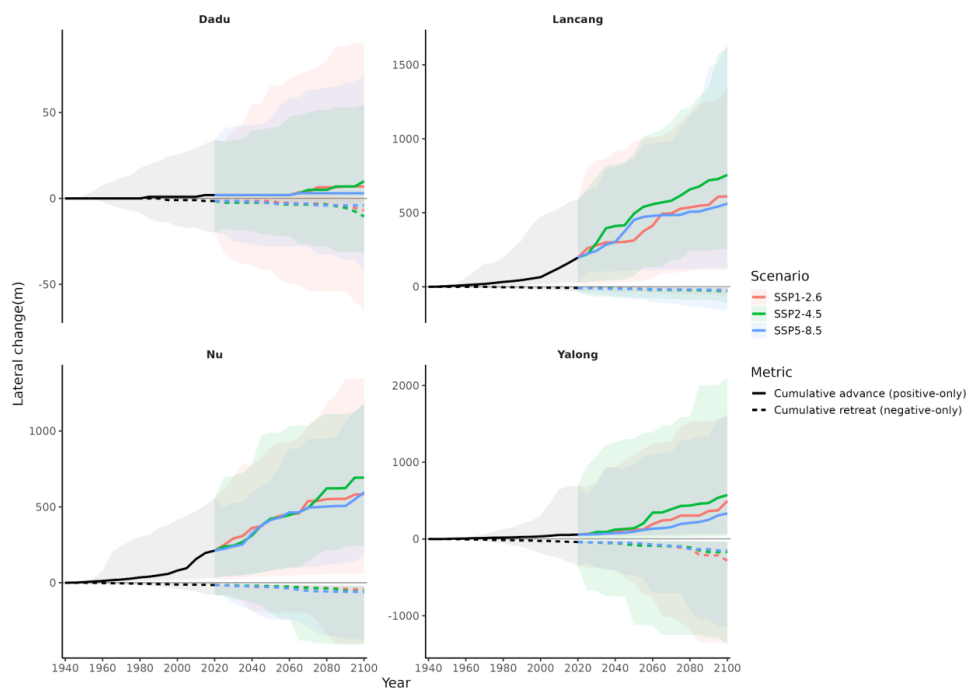
354 3 Results

355 3.1 Lateral treeline dynamics during the historical period

356 During the historical period from 1940 to 2020, all rivers showed gradual lateral shifts of the treeline, although
357 the magnitude of change differed markedly among river systems (Fig. 3). Based on the mean cumulative
358 trajectories, the Dadu River remained nearly stable, with only very small cumulative advance and retreat
359 throughout this period. In contrast, the Lancang River and Nu River exhibited much stronger cumulative advances,
360 both reaching about 200 m by 2020. In these two rivers, the increase became more pronounced after around 1980,
361 although the overall trend remained progressive rather than abrupt. The Yalong River showed an intermediate
362 pattern, with cumulative advance reaching approximately 60 m by 2020 and a smoother trajectory than those of
363 the Lancang River and Nu River.

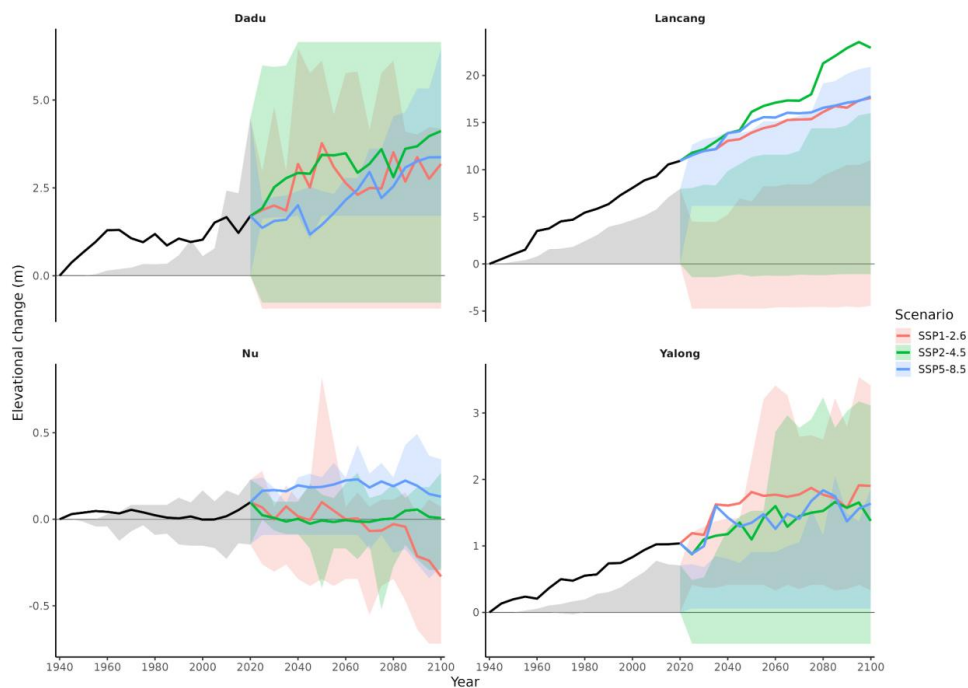
364 At the same time, all rivers showed weak but persistent cumulative retreat during the historical period. Although
365 retreat remained much smaller than advance, its presence indicates that lateral treeline dynamics were not
366 expressed as a purely one directional expansion. Instead, the historical period was characterized by modest but
367 bidirectional boundary change, with advance dominating over retreat in all four rivers.

368 The 25–75% quantile bands (Fig. 3) showed that uncertainty differed substantially among rivers. Historical
369 variability was relatively small in the Dadu River, but much larger in the Lancang River, Nu River, and Yalong
370 River, indicating that even under the same historical forcing, the magnitude of simulated lateral shift varied
371 strongly among simulation runs.



372
373
374
375
376

Figure 3. Cumulative lateral treeline advances and retreat across rivers under SSP scenarios, with 25–75% quantile bands, for 1940–2100 CE. Solid lines show cumulative advance (positive-only), and dashed lines show cumulative retreat (negative-only). The historical period (1940–2020) is merged and shown in black, whereas future trajectories (2020–2100) are shown separately for SSP1-2.6, SSP2-4.5, and SSP5-8.5



377



378 **Figure 4.** Treeline elevational change across rivers under SSP scenarios, with 25–75% quantile bands, for 1940–2100 CE. The
379 historical period (1940–2020) is merged and shown in black, whereas future trajectories (2020–2100) are shown separately
380 for SSP1-2.6, SSP2-4.5, and SSP5-8.5

381

382 **3.2 Lateral treeline dynamics during the future period**

383 During the future period from 2020 to 2100, lateral treeline trajectories became increasingly divergent among
384 scenarios and river systems (Fig. 4). All rivers showed stronger lateral shifts than during the historical period,
385 indicating a transition to a more dynamic phase of treeline change. In most rivers, the mean cumulative advance
386 reached around 500 m by 2100. Among the three scenarios, SSP2-4.5 generally produced the strongest mean
387 cumulative advance, with maxima reaching about 560 m, whereas SSP1-2.6 and SSP5-8.5 showed lower maxima
388 of approximately 438 m and 385 m, respectively.

389 The largest increases occurred in the Lancang River and Nu River, where the mean cumulative advance reached
390 about 446 m and 412 m by 2100. In both rivers, the increase was rapid and sustained throughout the future period.
391 The Yalong River also showed substantial advance, reaching about 409 m by 2100, but its trajectory exhibited a
392 more abrupt acceleration around the 2060s compared with those of the Lancang River and Nu River. By contrast,
393 the Dadu River remained much more stable, with the mean cumulative advance reaching only about 5 m by 2100,
394 indicating a much weaker future response relative to the other rivers.

395 Mean cumulative retreat also increased across all rivers during the future period, although its magnitude remained
396 lower than that of cumulative advance. By 2100, retreat values ranged from about 6 to 160 m, with particularly
397 clear increases under SSP1-2.6 and SSP2-4.5 in some river systems. The 25–75% quantile bands showed that
398 uncertainty widened substantially after 2020, especially in the Lancang River, Nu River, and Yalong River (Fig.
399 4). This indicated that future lateral treeline change is characterized not only by stronger average expansion, but
400 also by greater variation among simulation runs. Overall, the results showed that lateral treeline dynamics shift
401 from a relatively slow and convergent historical pattern to a faster and increasingly divergent future pattern.

402 **3.3 Elevational treeline dynamics across river systems**

403 Elevational changes in treeline position differed markedly among river systems (Fig. 4). During the historical
404 period from 1940 to 2020, treeline elevation changed only gradually in most rivers, but the magnitude of change
405 varied substantially. The strongest elevational increase occurred in the Lancang River, where treeline elevation
406 rose continuously over the 80-year period and had already increased by more than 10 m by around 2020. In
407 contrast, the Dadu River and Yalong River showed only modest upward changes, with cumulative increases of
408 roughly 1–2 m during the same period. The Nu River exhibited the weakest elevational response, remaining close
409 to stable with only slight fluctuations.

410 During the future period from 2020 to 2100, scenario specific divergence became more evident. The Lancang
411 River maintained the strongest upward trend under all future scenarios, with the largest increase under SSP2-4.5
412 and a cumulative elevational gain exceeding 20 m by 2100. The Dadu River also continued to rise, but with a
413 much smaller magnitude and stronger variation among scenarios. The Yalong River showed an intermediate
414 response, with continued but moderate elevational increases under all scenarios. By contrast, the Nu River

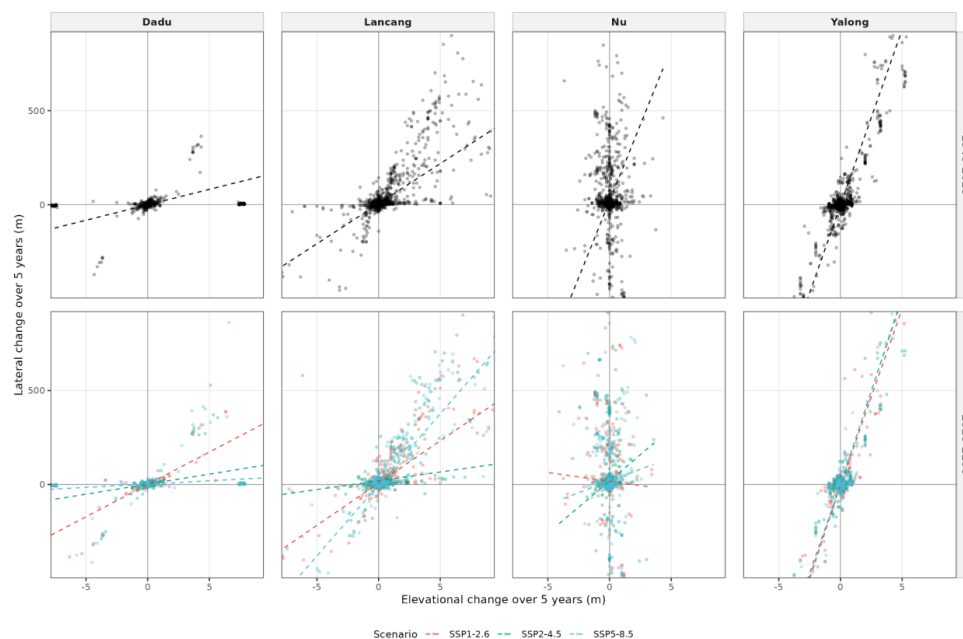


415 remained the least responsive in elevational terms, with only minor changes and a slight negative trend under
 416 SSP1-2.6 toward the end of the century.

417 The 25–75% quantile bands showed that uncertainty differed substantially among rivers and became greater after
 418 2020(Fig. 4). Quantile ranges were especially large in the Dadu River and Lancang River, indicating considerable
 419 variation among simulation runs in future elevational responses. In the Yalong River, the quantile bands also
 420 showed a broader range during the future period, although the mean upward trend remained moderate. By contrast,
 421 the Nu River showed relatively small mean changes but still displayed a notable spread around zero, indicating
 422 that its future elevational response remained weak and uncertain rather than strongly directional. Overall, clear
 423 spatial differences were observed in treeline elevational change across the Hengduan Mountains, with the Lancang
 424 River showing the largest increase, the Dadu Rive and Yalong River showing moderate increases, and the Nu
 425 River showing the smallest overall change.

426 We compared lateral treeline change with elevational treeline change across 5-year windows (Fig. 5). The
 427 relationship differed markedly among river systems, with the strongest positive coupling in the Lancang River,
 428 almost no elevational response in the Nu River, and intermediate patterns in the Dadu River and Yalong River.

429



430

431 **Figure 5.** Relationship between lateral and elevational treeline change across four river systems over 5-year windows.
 432 Historical windows (1940-2020) are shown in black, and future windows (2020-2100) are shown separately for SSP1-2.6,
 433 SSP2-4.5, and SSP5-8.5. Panels are arranged by river corridor, with the upper row showing the historical period and the lower
 434 row showing the future period. Each point represents one 5-year window. Axis ranges were limited to improve the visibility
 435 of the main point distributions; extreme values outside the plotting range are not shown. Dashed lines indicate fitted linear



436 relationships and should be interpreted as visual summaries.

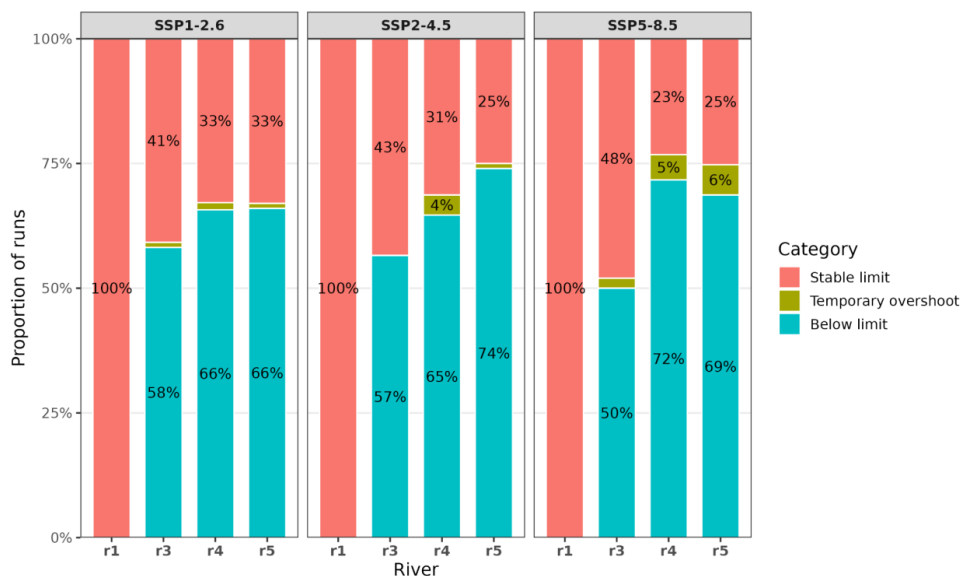
437 **3.4 Treeline states across rivers and scenarios**

438 To further compare river specific differences in treeline behaviour, we summarized the final simulated treeline
 439 states into three categories: runs that kept advancing to the predefined upper limit (“Stable limit”), runs that
 440 reached the limit briefly but then retreated (“Temporary overshoot”), and runs that never reached the limit (“Below
 441 limit”) (Fig. 6).

442 The Dadu River was the most consistent case. Under all three SSPs, 100% of runs remained in the category “Stable
 443 limit”, indicating that all versions reached and maintained the predefined upper limit. In contrast, the other three
 444 rivers were dominated by runs that never reached the limit. In the Lancang River, about 50–58% of runs belonged
 445 to the category “Below limit”, whereas 41–48% remained in “Stable limit”. In the Nu River and Yalong River,
 446 the dominance of “Below limit” was even clearer, accounting for about 65–74% of runs depending on scenario,
 447 while only about 23–33% remained in “Stable limit”.

448 The category “Temporary overshoot” was always small, generally ranging from 0 to 6%. This indicated that
 449 temporary reaching of the upper limit followed by retreat occurred only in a few runs. Dadu River was consistently
 450 able to maintain the upper limit, whereas most runs in Lancang River, Nu River, and Yalong River did not reach
 451 that limit by the end of the simulation.

452



453

454 **Figure 6.** Treeline state composition across rivers and scenarios. Stacked bars show the proportion of simulation runs in three
 455 treeline states: Stable limit, Temporary overshoot, and Below limit. Bars are grouped by future scenarios (SSP1-2.6, SSP2-
 456 4.5, and SSP5-8.5). River codes correspond to the four study corridors: r1 = Dadu River, r3 = Lancang River, r4 = Nu River,



457 and $r5$ = Yalong River. Percentages within each river \times scenario sum to 100%.

458 **4 Discussion**

459 **4.1 Historical and future treeline lateral dynamics**

460 During the historical period (1940–2020), simulated forest treeline dynamics were generally slow, but differed
461 markedly among river systems. The Dadu River showed only weak cumulative advance and retreat, indicating a
462 comparatively stable forest boundary, whereas the Lancang and Nu rivers already exhibited substantial cumulative
463 advance before 2020, and the Yalong River showed intermediate but clearly dynamic behaviour. This pattern is
464 consistent with the broader view that historical treeline responses are spatially heterogeneous and are not always
465 expressed as simple upslope shifts (Harsch et al., 2009; Schickhoff et al., 2015). In the Hengduan Mountains,
466 recent landscape observations similarly showed that treeline position often remained broadly stable while
467 vegetation cover increased across most treeline areas, suggesting that historical responses may first appear as
468 structural infilling or boundary adjustment rather than obvious positional displacement (Zou et al., 2022).

469
470 The contrast among river corridors is ecologically plausible given the strong environmental heterogeneity of the
471 Hengduan Mountains. Differences in valley morphology, disturbance history, vegetation composition, riverine
472 connectivity, and local topographic setting may all contribute to river-specific forest boundary dynamics. For
473 example, forest change in the upper Dadu River watershed has been influenced by deforestation, rehabilitation,
474 and degradation processes, whereas vegetation patterns in the Lancang and Nu valleys are strongly shaped by
475 riverine landscapes, topographic gradients, and local environmental filtering (Yan et al., 2005; Li et al., 2012; Liu
476 et al., 2014; Zhao et al., 2023). Previous phylogeographic work also suggests that the Yalong River has played an
477 important role in plant dispersal and divergence in the Hengduan Mountains, which is consistent with the relatively
478 dynamic boundary behaviour simulated here (Jian et al., 2016). Altogether, the historical results suggest that forest
479 treeline dynamics in the Hengduan Mountains are better understood as modest but spatially heterogeneous forest
480 boundary changes, rather than as a single regionally homogeneous treeline shift.

481
482 After 2020, simulated treeline dynamics became much more active across all four river systems, with stronger
483 cumulative advance and clearer divergence among future scenarios. This transition from a relatively constrained
484 historical phase to a more dynamic future phase agrees with treeline studies showing that warming can intensify
485 treeline and ecotone dynamics, although the magnitude and direction of change remain strongly modulated by
486 ecological processes and landscape context (Dullinger et al., 2004; Zheng et al., 2021). In our simulations, the
487 Lancang and Nu rivers showed the strongest cumulative advance, the Dadu River remained weakly responsive,
488 and the Yalong River displayed both substantial advance and retreat. This indicates that future forest treeline
489 change cannot be reduced to a simple monotonic expansion signal. Instead, simultaneous advance and retreat
490 along different boundary segments, especially in the Yalong River, suggest ongoing reorganization within the
491 treeline ecotone.

492
493 Such an interpretation is consistent with recent work emphasizing that future treeline responses are likely to
494 involve not only positional change, but also ecotone restructuring, forest expansion into alpine habitats, and
495 nonlinear responses driven by dispersal, density dependence, and local site conditions (Kruse et al., 2023; Kumar
496 and Khanduri, 2024). More generally, future vegetation projections from the Himalaya and other mountain regions
497 indicate that suitable habitats and forest boundaries at higher elevations may shift and reorganize under continued
498 warming, often with strong scenario-dependent divergence and important consequences for alpine habitat
499 availability (Chhetri et al., 2018; Barredo et al., 2020). Therefore, our results support the view that future treeline
500 dynamics in the Hengduan Mountains will be characterized not simply by upward or outward expansion, but by
501 increasingly divergent and spatially heterogeneous forest boundary dynamics across river corridors.

502
503 The scenario responses further suggest that warming intensity alone did not determine lateral treeline expansion.
504 Warmer conditions are generally expected to promote treeline advance because low temperature is widely
505 regarded as a major constraint on tree establishment and persistence near upper treeline limits (Körner, 2021).



506 Many studies have shown that warming can facilitate upward forest expansion or woody encroachment into open
507 alpine and subalpine habitats (Albert et al., 2008; Piccinelli et al., 2020; Wang et al., 2022). However, our
508 simulations did not show a simple monotonic increase from SSP1-2.6 to SSP5-8.5. Instead, SSP2-4.5 produced
509 the strongest cumulative advance in several cases, particularly in the Lancang, Nu, and Yalong rivers. This pattern
510 suggests that realized treeline expansion in the Hengduan Mountains was shaped by the interaction between
511 climate forcing and local ecological constraints, rather than by warming intensity alone.

512

513 Similar conclusions have been reached in other mountain systems, where upslope forest advance can remain
514 strongly constrained by topographic conditions even under warming (Macias-Fauria et al., 2013). Studies from
515 mountain grassland and treeline ecotone systems also show that woody encroachment depends on land-use legacy,
516 colonization opportunities, and local site conditions, in addition to climate (Albert et al., 2008; Piccinelli et al.,
517 2020). Species-specific responses may further complicate this relationship, as dominant Himalayan treeline
518 species can respond differently to climate change (Mainali et al., 2020). From this perspective, intermediate
519 scenarios may remain closer to the suitable climatic space of particular treeline-forming species, whereas stronger
520 warming may generate mixed or locally constrained responses rather than continuous lateral expansion.

521

522 **4.2 River specific differences in elevational treeline change**

523 Elevational treeline change added an important constraint to the interpretation of lateral treeline dynamics.
524 Although lateral forest expansion was evident in several river corridors, it was not always accompanied by a
525 comparable upward shift in treeline elevation. During the historical period, most river corridors showed only
526 limited elevational advance. The Lancang River was the main exception, showing a sustained increase in treeline
527 elevation, whereas the Dadu and Yalong rivers showed only modest gains and the Nu River remained nearly stable.
528 This contrast suggests that lateral reorganization of the forest boundary and upslope displacement of the upper
529 treeline represent related but distinct dimensions of treeline change.

530 Future projections reinforced this distinction. Elevational trajectories became more differentiated among river
531 corridors, with the Lancang River maintaining the clearest upward trend, the Dadu and Yalong rivers showing
532 more moderate increases, and the Nu River remaining weakly responsive, including a slight decline under SSP1-
533 2.6 near the end of the century. These results suggest that warming may amplify existing differences in elevational
534 sensitivity, but does not produce a uniform upslope response across the Hengduan Mountains. Positive coupling
535 between lateral and elevational change was most evident in the Lancang and Yalong rivers, whereas the Nu River
536 showed weak elevational change despite lateral dynamics. Such river-specific differences likely reflect variation
537 in topographic configuration, local terrain constraints, regeneration conditions, and species interactions, all of
538 which can moderate treeline responses to climate warming (Schickhoff et al., 2015; Liang et al., 2016; Wang et
539 al., 2022).

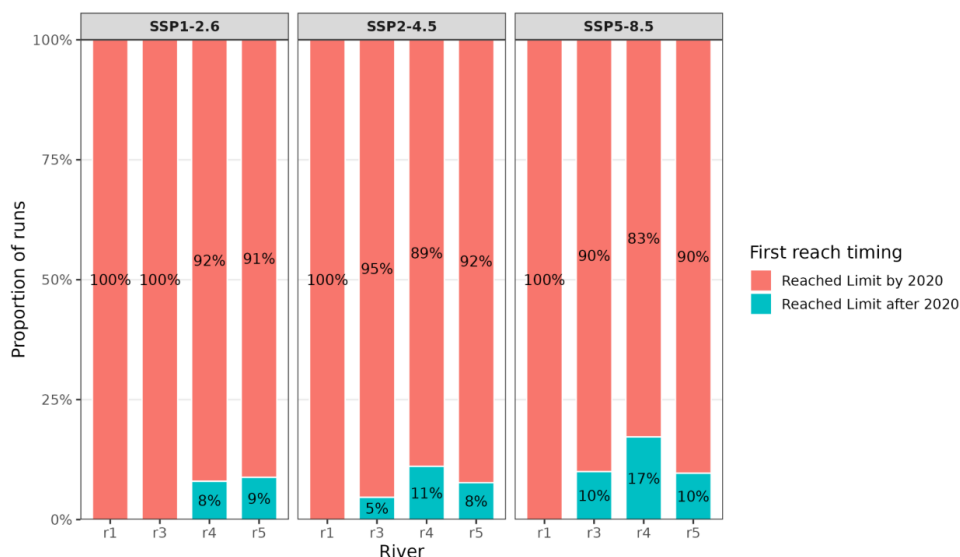
540 These findings support a cautious interpretation of treeline advance. Lateral change describes the horizontal
541 redistribution and infilling of forest along the treeline ecotone, whereas elevational change indicates whether the
542 upper forest boundary has shifted upslope. In this study, these two dimensions were coupled in some river
543 corridors but were not interchangeable. This distinction is consistent with recent evidence that increased tree
544 density within treeline ecotones can be partly decoupled from upward movement of the upper treeline (Feuillet et
545 al., 2020; Shi et al., 2022). Field observations from the Central Alps similarly show that recent increases in tree
546 abundance may largely reflect infilling below or near the former treeline rather than true upward advance of the



547 upper boundary (Frei et al., 2023). Therefore, fitted relationships between lateral and elevational change should
 548 be interpreted as visual summaries rather than evidence of a single, consistent mechanism. This distinction is
 549 important for assessing future alpine habitat vulnerability, because forest expansion within the treeline ecotone
 550 may continue to reduce alpine shrubland and meadow habitats even where mean treeline elevation changes only
 551 weakly.

552 **4.3 Treeline invasion potential and implications for alpine habitat loss**

553 The upper limit results suggested that most river corridors remained relatively conservative in terms of treeline
 554 invasion potential. In the majority of simulations, especially outside the Dadu River, treeline advance did not
 555 reach the predefined upper limit, indicating that forest expansion into the full treeline tundra ecotone was often
 556 incomplete by the end of the simulation period. This suggests that future treeline advance in the Hengduan
 557 Mountains may be substantial, but in most corridors, it is still unlikely to occupy all potentially colonizable space
 558 within the simulated domain. Such a pattern is consistent with earlier studies showing that warming does not
 559 automatically translate into full or rapid invasion of alpine habitats, because realized expansion is often
 560 constrained by recruitment, microsite availability, land use history, and topographic setting (Albert et al., 2008;
 561 Macias-Fauria et al., 2013; Piccinelli et al., 2020). The Dadu River represented a notable exception, as simulated
 562 treelines more frequently reached and maintained the upper limit. However, this result should be interpreted
 563 cautiously. It may reflect not only a stronger effective response in this corridor, but also the comparatively shorter
 564 simulation extent, which makes the predefined limit easier to attain within the current model setup. The apparent
 565 invasion potential of a corridor therefore depends not only on ecological response, but also to some degree on
 566 how the simulation area is defined.



567

568 **Figure 7.** Timing of first reaching the predefined upper limit among simulation runs that reached the limit at least once. Bars
 569 show the proportion of runs within each river corridor and future scenario, separated into runs that first reached the limit by
 570 2020 and runs that first reached it after 2020. Percentages within each river and scenario sum to 100% among runs that ever



571 reached the limit. River codes indicate r1 = Dadu River, r3 = Lancang River, r4 = Nu River, and r5 = Yalong River.

572 An additional result is that, even when potential invasions occurred, they usually took place early rather than being
573 newly generated under future scenarios (Fig. 7). Among runs that ever reached the upper limit, the first attainment
574 occurred predominantly before 2020 in all rivers and scenarios. Reaching the limit for the first time after 2020
575 remained rare and generally accounted for only a small fraction of runs. This indicates that future climate forcing
576 more often modified or extended an already established invasion tendency than initiated a completely new one.
577 Current ecotone structure and pre-existing demographic conditions can strongly shape how treelines respond to
578 subsequent warming (Camarero et al., 2017), which may explain why scenario effects were secondary to the
579 broader contrast between corridors that already had the potential to reach the limit and those that remained
580 constrained throughout the simulation.

581 These results have direct implications for alpine habitat loss, but the implication is not a simple uniform loss
582 across all river corridors. Climate based projections from European mountains suggest that alpine tundra climate
583 space may contract substantially under future warming, with stronger losses under higher warming levels (Barredo
584 et al., 2020). Our results point in a similar general direction, but they also suggest that habitat loss in the Hengduan
585 Mountains is likely to be uneven. Corridors with higher invasion potential may face greater pressure from forest
586 expansion into the treeline tundra ecotone, whereas corridors with weak or incomplete advance may retain more
587 alpine habitat within the simulated period. Therefore, future alpine habitat vulnerability in this region should be
588 interpreted as spatially heterogeneous and corridor specific, rather than as a uniform consequence of regional
589 warming.

590 **5 Conclusions**

591 This study modified and used the spatially explicit individual based model LAVESI to examine how treeline
592 dynamics respond to historical and future climate forcing along major river corridors in the Hengduan Mountains.
593 The results showed that treeline dynamics were already detectable during the historical period, but their magnitude
594 and timing differed strongly among rivers. Lateral advance remained limited before 2020 in most systems, with
595 the Dadu River showing only weak boundary displacement, the Yalong River showing an intermediate response,
596 and the Lancang and Nu rivers showing the clearest cumulative advance. In elevational terms, the Lancang River
597 displayed the strongest historical upward shift, whereas the Nu River remained nearly stable. These results indicate
598 that historical to modern treeline change along river corridors was gradual rather than abrupt, and that ecological
599 processes and local environmental settings strongly mediated how climate forcing was translated into boundary
600 movement.

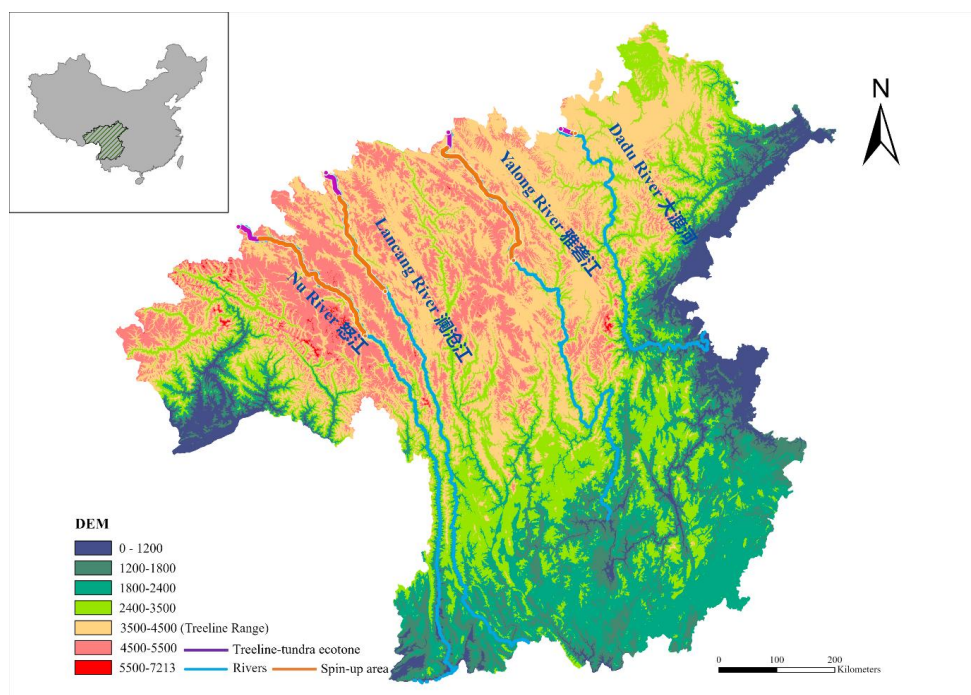
601 The future simulations showed that river specific migration trajectories will diverge more strongly after 2020
602 under different climate change scenarios. In most rivers, lateral advance accelerated during the future period, with
603 SSP2-4.5 generally producing relatively high cumulative expansion. The Lancang River and Nu River showed
604 the greatest future lateral advance, whereas the Dadu River remained comparatively stable and the Yalong River
605 combined substantial advance with substantial retreat, indicating boundary reorganization rather than simple one
606 directional expansion. Elevational change followed a related but not identical pattern: the Lancang River
607 maintained the strongest upward shift under all scenarios, the Dadu and Yalong rivers showed moderate increases,



608 and the Nu River remained the least responsive, with only weak changes and a slight negative trend under SSP1-
609 2.6. Thus, future treeline migration in the Hengduan Mountains is unlikely to follow a single regional pattern, but
610 will instead depend strongly on river specific ecological and topographic settings.

611 Furthermore, these findings suggest that future treeline advance in the Hengduan Mountains is likely to be uneven
612 across river corridors. The Lancang River showed a relatively strong and sustained response in both lateral and
613 elevational dimensions, indicating a higher potential for forest expansion into the treeline tundra ecotone. In
614 contrast, the Dadu River and especially the Nu River in elevational terms showed more constrained responses.
615 Alpine habitat loss is therefore unlikely to occur evenly across the region. The greatest vulnerability may occur
616 where lateral expansion is strong, upslope movement is sustained, and simulated treeline advance approaches the
617 available treeline tundra ecotone. In general, alpine habitat vulnerability should be evaluated at the corridor scale
618 rather than inferred from a single regional treeline response.

619 Appendix A



620 **Figure A1.** Digital elevation model of the study area showing elevation zones, the treeline range, and major river systems.
621 The simulated area along river systems was marked with orange and purple line, which represents spin-up area and treeline-
622 tundra ecotone respectively.
623

624 Code and Data availability

625 The source code of host model is publicly available from github <https://github.com/StefanKruse/LAVESI>. The
626 updated version created in this study will receive a tag and final publication at Zenodo after acceptance of the



627 manuscript for publication (current commit
628 <https://github.com/StefanKruse/LAVESI/tree/dd10208a9923b0310e5b8a9210951132de01ce23>).
629

630 **Supplement link**

631 Check the file link.

632 **Author contributions**

633 LW: Conceptualisation; methodology; software; validation; formal analysis; investigation; resources; data
634 curation; writing original draft; writing review & editing; visualisation. SK: Conceptualisation; methodology;
635 software; validation; formal analysis; investigation; resources; data curation; writing review & editing;
636 supervision; project administration; funding acquisition. JN: Writing review & editing; supervision. XC: Writing
637 review & editing.
638

639 **Competing interests**

640 The contact author has declared that none of the authors has any competing interests.

641

642

643 **Acknowledgements**

644 The authors sincerely thank members of Jian Ni's research group at Zhejiang Normal University for their
645 assistance with sample and data collection and species identification during the field surveys conducted in 2023
646 and 2024. The authors also thank Yanrong Zhang from the Alfred Wegener Institute, Helmholtz Centre for Polar
647 and Marine Research, for fieldwork support.

648 **Financial support**

649 This research has been supported by China Scholarship Council (grant 202208330012 to Linfeng Wei).

650

651

652

653 **References**

654 Antonelli, A., Kissling, W. D., Flantua, S. G. A., Bermúdez, M. A., Mulch, A., Muellner-Riehl, A. N., Kreft, H.,
655 Linder, H. P., Badgley, C., Fjeldså, J., Fritz, S. A., Rahbek, C., Herman, F., Hooghiemstra, H., and Hoorn, C.:
656 Geological and climatic influences on mountain biodiversity, *Nat. Geosci.*, 11, 718–725,
657 <https://doi.org/10.1038/s41561-018-0236-z>, 2018.



- 658 Bader, M. Y., Llambí, L. D., Case, B. S., Buckley, H. L., Toivonen, J. M., Camarero, J. J., Cairns, D. M., Brown,
659 C. D., Wiegand, T., and Resler, L. M.: A global framework for linking alpine treeline ecotone patterns to
660 underlying processes, *Ecography*, 44, 265–292, <https://doi.org/10.1111/ecog.05285>, 2021.
- 661 Barbeito, I., Dawes, M. A., Rixen, C., Senn, J., and Bebi, P.: Factors driving mortality and growth at treeline: a
662 30-year experiment of 92,000 conifers, *Ecology*, 93, 389–401, <https://doi.org/10.1890/11-0384.1>, 2012.
- 663 Barredo, J. I., Mauri, A., and Caudullo, G.: Alpine tundra contraction under future warming scenarios in Europe,
664 *Atmosphere*, 11, 698, <https://doi.org/10.3390/atmos11070698>, 2020.
- 665 Bobrowski, M., Gerlitz, L., and Schickhoff, U.: Modelling the potential distribution of *Betula utilis* in the
666 Himalaya, *Global Ecol. Conserv.*, 11, 69–83, <https://doi.org/10.1016/j.gecco.2017.04.003>, 2017.
- 667 Bobrowski, M., Weidinger, J., Schwab, N., and Schickhoff, U.: Searching for ecology in species distribution
668 models in the Himalayas, *Ecol. Model.*, 458, 109693, <https://doi.org/10.1016/j.ecolmodel.2021.109693>, 2021.
- 669 Camarero, J. J., Linares, J. C., García-Cervigón, A. I., Batllori, E., Martínez, I., and Gutiérrez, E.: Back to the
670 future: The responses of alpine treelines to climate warming are constrained by the current ecotone structure,
671 *Ecosystems*, 20, 683–700, <https://doi.org/10.1007/s10021-016-0046-3>, 2017.
- 672 Chen, D. L., Xu, B. Q., Yao, T. D., Guo, Z. T., Cui, P., Chen, F. H., Zhang, R. H., Zhang, X. Z., Zhang, Y. L.,
673 Fan, J., Hou, Z. Q., and Zhang, T. H.: Assessment of past, present and future environmental changes on the Tibetan
674 Plateau, *Chin. Sci. Bull.*, 60, 3025–3035, <https://doi.org/10.1360/N972014-01370>, 2015.
- 675 Chhetri, P. K., Gaddis, K. D., and Cairns, D. M.: Predicting the suitable habitat of treeline species in the Nepalese
676 Himalayas under climate change, *Mt. Res. Dev.*, 38, 201–213, <https://doi.org/10.1659/MRD-JOURNAL-D-17-00071.1>, 2018.
- 677
- 678 Corenblit, D., Tabacchi, E., Steiger, J., and Gurnell, A. M.: Reciprocal interactions and adjustments between
679 fluvial landforms and vegetation dynamics in river corridors: A review of complementary approaches, *Earth-Sci.
680 Rev.*, 84, 56–86, <https://doi.org/10.1016/j.earscirev.2007.05.004>, 2007.
- 681 Di Musciano, M., Di Cecco, V., Bartolucci, F., Conti, F., Frattaroli, A. R., and Di Martino, L.: Dispersal ability
682 of threatened species affects future distributions, *Plant Ecol.*, 221, 265–281, <https://doi.org/10.1007/s11258-020-01009-0>, 2020.
- 683
- 684 Ding, W. N., Ree, R. H., Spicer, R. A., and Xing, Y. W.: Ancient orogenic and monsoon-driven assembly of the
685 world's richest temperate alpine flora, *Science*, 369, 578–581, <https://doi.org/10.1126/science.abb4484>, 2020.
- 686 Dirnböck, T., Essl, F., and Rabitsch, W.: Disproportional risk for habitat loss of high-altitude endemic species
687 under climate change, *Glob. Change Biol.*, 17, 990–996, <https://doi.org/10.1111/j.1365-2486.2010.02266.x>, 2011.
- 688 Feuillet, T., Birre, D., Milian, J., Godard, V., Clauzel, C., and Serrano-Notivol, R.: Spatial dynamics of alpine
689 tree lines under global warming: What explains the mismatch between tree densification and elevational upward
690 shifts at the tree line ecotone?, *J. Biogeogr.*, 47, 1056–1068, <https://doi.org/10.1111/jbi.13779>, 2020.
- 691 Frei, E. R., Barbeito, I., Erdle, L. M., Leibold, E., and Bebi, P.: Evidence for 40 years of treeline shift in a central
692 Alpine valley, *Forests*, 14, 412, <https://doi.org/10.3390/f14020412>, 2023.
- 693 Gao, B. C., Fang, W. P., Kong, X. X., Xu, J. M., Guan, Z. T., Yang, J. L., Xiong, J. H., Yi, T. P., Wu, Y. T., Tan,
694 and Z. M.: *Flora of Sichuan*, Sichuan People's Publishing House, Chengdu, 1981.
- 695 Gloy, J., Herzschuh, U., and Kruse, S.: Evolutionary adaptation of trees and modelled future larch forest extent in
696 Siberia, *Ecol. Model.*, 478, 110278, <https://doi.org/10.1016/j.ecolmodel.2023.110278>, 2023.



- 697 Greenwood, S., Chen, J. C., Chen, C. T., and Jump, A. S.: Temperature and sheltering determine patterns of
698 seedling establishment in an advancing subtropical treeline, *J. Veg. Sci.*, 26, 711–721,
699 <https://doi.org/10.1111/jvs.12269>, 2015.
- 700 Grissino-Mayer, H. D. and Fritts, H. C.: The International Tree-Ring Data Bank: an enhanced global database
701 serving the global scientific community, *Holocene*, 7, 235–238, <https://doi.org/10.1177/095968369700700212>,
702 1997.
- 703 Gurnell, A. M., Corenblit, D., García de Jalón, D., González del Tánago, M., Grabowski, R. C., O’Hare, M. T.,
704 and Szewczyk, M.: A conceptual model of vegetation-hydrogeomorphology interactions within river corridors,
705 *River Res. Appl.*, 32, 142–163, <https://doi.org/10.1002/rra.2928>, 2016.
- 706 Gustafson, A., Miller, P. A., Björk, R. G., Olin, S., and Smith, B.: Nitrogen restricts future sub-arctic treeline
707 advance in an individual-based dynamic vegetation model, *Biogeosciences*, 18, 6329–6345,
708 <https://doi.org/10.5194/bg-18-6329-2021>, 2021.
- 709 Hamid, M., Gulzar, A., Dar, F. A., Singh, C. P., Malik, A. H., Kamili, A. N., and Khuroo, A. A.: Microclimate
710 heterogeneity modulates fine-scale edaphic and vegetation patterns on the Himalayan treelines: implications under
711 climate change, *Agr. Forest Meteorol.*, 341, 109688, <https://doi.org/10.1016/j.agrformet.2023.109688>, 2023.
- 712 Harris, I., Osborn, T. J., Jones, P., and Lister, D.: Version 4 of the CRU TS monthly high-resolution gridded
713 multivariate climate dataset, *Sci. Data*, 7, 109, <https://doi.org/10.1038/s41597-020-0453-3>, 2020.
- 714 Harsch, M. A., Hulme, P. E., McGlone, M. S., and Duncan, R. P.: Are treelines advancing? A global meta-analysis
715 of treeline response to climate warming, *Ecol. Lett.*, 12, 1040–1049, <https://doi.org/10.1111/j.1461-0248.2009.01355.x>, 2009.
- 717 He, Y., Xiong, Q., Yu, L., Yan, W., and Qu, X.: Impact of climate change on potential distribution patterns of
718 alpine vegetation in the Hengduan Mountains region, China, *Mt. Res. Dev.*, 40, R16–R26,
719 <https://doi.org/10.1659/MRD-JOURNAL-D-20-00010.1>, 2020.
- 720 Hersbach, H., Bell, B., Berrisford, P., Hirahara, S., Horányi, A., Muñoz-Sabater, J., Nicolas, J., Peubey, C., Radu,
721 R., Schepers, D., Simmons, A., Soci, C., Abdalla, S., Abellan, X., Balsamo, G., Bechtold, P., Biavati, G., Bidlot,
722 J., Bonavita, M., De Chiara, G., Dahlgren, P., Dee, D., Diamantakis, M., Dragani, R., Flemming, J., Forbes, R.,
723 Fuentes, M., Geer, A., Haimberger, L., Healy, S., Hogan, R. J., Hólm, E., Janisková, M., Keeley, S., Laloyaux,
724 P., Lopez, P., Lupu, C., Radnoti, G., de Rosnay, P., Rozum, I., Vamborg, F., Villaume, S., and Thépaut, J.-N.:
725 The ERA5 global reanalysis, *Q. J. Roy. Meteor. Soc.*, 146, 1999–2049, <https://doi.org/10.1002/qj.3803>, 2020.
- 726 Ho, Y.F., Grohmann, C. H., Lindsay, J. B., Reuter, H. I., Cavalli, M., and Hengl, T.: GEDTM30: global ensemble
727 digital terrain model at 30 m and derived multiscale terrain variables, *PeerJ*, 13, e19673,
728 <https://doi.org/10.7717/peerj.19673>, 2025.
- 729 Holešťová, A. and Douda, J.: Plant species over-occupancy indicates river valleys are natural corridors for
730 migration, *Plant Ecol.*, 223, 71–83, <https://doi.org/10.1007/s11258-021-01191-9>, 2022.
- 731 Holtmeier, F.-K. and Broll, G.: Sensitivity and response of northern hemisphere altitudinal and polar treelines to
732 environmental change at landscape and local scales, *Global Ecol. Biogeogr.*, 14, 395–410,
733 <https://doi.org/10.1111/j.1466-822X.2005.00168.x>, 2005.
- 734 Huo, C., Cheng, G., Lu, X., and Fan, J.: Simulating the effects of climate change on forest dynamics on Gongga
735 Mountain, Southwest China, *J. Forest Res.*, 15, 176–185, <https://doi.org/10.1007/s10310-009-0173-1>, 2010.
- 736 Integrated Scientific Expedition to Qinghai-Tibet Plateau, Chinese Academy of Sciences: *Flora Xizangica*, 5
737 volumes, Science Press, Beijing, 1983–1987.



- 738 Integrated Scientific Expedition to Qinghai-Tibet Plateau, Chinese Academy of Sciences: Physical Geography of
739 Hengduan Mountains, Science Press, Beijing, 1997.
- 740 Jin, Y., Yang, L., Hu, X., Yang, C., Xia, H., Hou, Y., Wu, K., Shi, S., Mao, X., and Ni, J.: HDM-Plot: a plot
741 dataset of plant communities across three-dimensional zonal vegetation in the Hengduan Mountains, southwestern
742 China, *Earth Syst. Sci. Data Discuss.* [preprint], <https://doi.org/10.5194/essd-2026-204>, 1 April 2026.
- 743 Kapsch, M.-L., Mikolajewicz, U., Ziemer, F., and Schannwell, C.: Ocean response in transient simulations of the
744 last deglaciation dominated by underlying ice-sheet reconstruction and method of meltwater distribution, *Geophys.*
745 *Res. Lett.*, 49, e2021GL096767, <https://doi.org/10.1029/2021GL096767>, 2022.
- 746 Körner, C.: The cold range limit of trees, *Trends Ecol. Evol.*, 36, 979–989,
747 <https://doi.org/10.1016/j.tree.2021.06.011>, 2021.
- 748 Kruse, S., Gerdes, A., Kath, N. J., Epp, L. S., Stoof-Leichsenring, K. R., Pestryakova, L. A., and Herzsuh, U.:
749 Dispersal distances and migration rates at the arctic treeline in Siberia – a genetic and simulation-based study,
750 *Biogeosciences*, 16, 1211–1224, <https://doi.org/10.5194/bg-16-1211-2019>, 2019.
- 751 Kruse, S., Stuenzi, S. M., Boike, J., Langer, M., Gloy, J., and Herzsuh, U.: Novel coupled permafrost–forest
752 model (LAVESI–CryoGrid v1.0) revealing the interplay between permafrost, vegetation, and climate across
753 eastern Siberia, *Geosci. Model Dev.*, 15, 2395–2422, <https://doi.org/10.5194/gmd-15-2395-2022>, 2022.
- 754 Kruse, S. and Herzsuh, U.: Regional opportunities for tundra conservation in the next 1000 years, *eLife*, 11,
755 e75163, <https://doi.org/10.7554/eLife.75163>, 2022.
- 756 Kruse, S., Wieczorek, M., Jeltsch, F., and Herzsuh, U.: Treeline dynamics in Siberia under changing climates
757 as inferred from an individual based model for *Larix*, *Ecol. Model.*, 338, 101–121,
758 <https://doi.org/10.1016/j.ecolmodel.2016.08.003>, 2016.
- 759 Kumar, S. and Khanduri, V. P.: Impact of climate change on the Himalayan alpine treeline vegetation, *Heliyon*,
760 10, e40797, <https://doi.org/10.1016/j.heliyon.2024.e40797>, 2024.
- 761 Kunming Institute of Botany, Chinese Academy of Sciences: Flora of Yunnan, 21 volumes, Science Press, Beijing,
762 1977–2006.
- 763 Li, J., Dong, S., Peng, M., Li, X., and Liu, S.: Vegetation distribution pattern in the dam areas along middle-low
764 reach of Lancang-Mekong River in Yunnan Province, China, *Front. Earth Sci.*, 6, 283–290,
765 <https://doi.org/10.1007/s11707-012-0296-0>, 2012.
- 766 Li, P., Zhu, W., Xie, Z., and Qiao, K.: Integration of multiple climate models to predict range shifts and identify
767 management priorities of the endangered *Taxus wallichiana* in the Himalaya–Hengduan Mountain region, *J.*
768 *Forest. Res.*, 31, 2255–2272, <https://doi.org/10.1007/s11676-019-01009-5>, 2020.
- 769 Li, X.H., Zhu, X.X., Niu, Y., and Sun, H.: Phylogenetic clustering and overdispersion for alpine plants along an
770 elevational gradient in the Hengduan Mountains region, southwest China, *J. Syst. Evol.*, 52, 280–288,
771 <https://doi.org/10.1111/jse.12027>, 2014.
- 772 Liang, E., Wang, Y., Piao, S., Lu, X., Camarero, J. J., Zhu, H., Zhu, L., Ellison, A. M., Ciais, P., and Peñuelas, J.:
773 Species interactions slow warming-induced upward shifts of treelines on the Tibetan Plateau, *P. Natl. Acad. Sci.*
774 *USA*, 113, 4380–4385, <https://doi.org/10.1073/pnas.1520582113>, 2016.
- 775 Lin, C., Yang, L., Zhou, R., Zhang, T., Han, Y., and Wang, Y.: Spatial pattern and environmental driving factors
776 of treeline elevations in Yulong Snow Mountain, China, *Forests*, 15, 1261, <https://doi.org/10.3390/f15071261>,
777 2024.



- 778 Meinshausen, M., Nicholls, Z. R. J., Lewis, J., Gidden, M. J., Vogel, E., Freund, M., Beyerle, U., Gessner, C.,
779 Nauels, A., Bauer, N., Canadell, J. G., Daniel, J. S., John, A., Krummel, P. B., Luderer, G., Meinshausen, N.,
780 Montzka, S. A., Rayner, P. J., Reimann, S., Smith, S. J., van den Berg, M., Velders, G. J. M., Vollmer, M. K., and
781 Wang, R. H. J.: The shared socio-economic pathway (SSP) greenhouse gas concentrations and their extensions to
782 2500, *Geosci. Model Dev.*, 13, 3571–3605, <https://doi.org/10.5194/gmd-13-3571-2020>, 2020.
- 783 Mienna, I. M., Speed, J. D. M., Klanderud, K., Austrheim, G., Næsset, E., and Bollandsås, O. M.: The relative
784 role of climate and herbivory in driving treeline dynamics along a latitudinal gradient, *J. Veg. Sci.*, 31, 403–413,
785 <https://doi.org/10.1111/jvs.12865>, 2020.
- 786 Naiman, R. J. and Décamps, H.: The ecology of interfaces: Riparian zones, *Annu. Rev. Ecol. Syst.*, 28, 621–
787 658, <https://doi.org/10.1146/annurev.ecolsys.28.1.621>, 1997.
- 788 Pauli, H., Gottfried, M., Dullinger, S., Abdaladze, O., Akhalkatsi, M., Alonso, J. L. B., Coldea, G., Dick, J.,
789 Erschbamer, B., Fernández Calzado, R., Ghosn, D., Holten, J. I., Kanka, R., Kazakis, G., Kollár, J., Larsson, P.,
790 Moiseev, P., Moiseev, D., Molau, U., Mesa, J. M., Nagy, L., Pelino, G., Puşcaş, M., Rossi, G., Stanisci, A.,
791 Syverhuset, A. O., Theurillat, J. P., Tomaselli, M., Unterluggauer, P., Villar, L., Vittoz, P., and Grabherr, G.:
792 Recent plant diversity changes on Europe’s mountain summits, *Science*, 336, 353–355,
793 <https://doi.org/10.1126/science.1219033>, 2012.
- 794 Piao, S. L., Zhang, X. Z., Wang, T., Liang, E. Y., Wang, S. P., Zhu, J. T., and Niu, B.: Responses and feedback
795 of the Tibetan Plateau’s alpine ecosystem to climate change, *Chin. Sci. Bull.*, 64, 2842–2855,
796 <https://doi.org/10.1360/TB-2019-0074>, 2019.
- 797 Pinheiro, J., Bates, D., and R Core Team: nlme: Linear and Nonlinear Mixed Effects Models, R package version
798 3.1-169, <https://CRAN.R-project.org/package=nlme>, <https://doi.org/10.32614/CRAN.package.nlme>, 2026.
- 799 R Core Team: R: A language and environment for statistical computing, R Foundation for Statistical Computing,
800 Vienna, Austria, <https://www.R-project.org/>, 2023.
- 801 Rees, W. G., Hofgaard, A., Boudreau, S., Cairns, D. M., Harper, K., Mamet, S., Mathisen, I., Swirad, Z., and
802 Tutubalina, O.: Is subarctic forest advance able to keep pace with climate change?, *Glob. Change Biol.*, 26, 3965–
803 3977, <https://doi.org/10.1111/gcb.15113>, 2020.
- 804 Riis, T., Kelly-Quinn, M., Aguiar, F. C., Manolaki, P., Bruno, D., Bejarano, M. D., Clerici, N., Fernandes, M. R.,
805 Franco, J. C., Pettit, N., Portela, A. P., Tammearg, O., Tammearg, P., Rodríguez-González, P. M., and Dufour,
806 S.: Global overview of ecosystem services provided by riparian vegetation, *BioScience*, 70, 501–
807 514, <https://doi.org/10.1093/biosci/biaa041>, 2020.
- 808 Rinaldo, A., Gatto, M., and Rodriguez, I.: River networks as ecological corridors: A coherent ecohydrological p
809 erspective, *Adv. Water Resour.*, 112, 27–58, <https://doi.org/10.1016/j.advwatres.2017.10.005>, 2018.
- 810 Rita, A., Saracino, A., Cieraad, E., Saulino, L., Zotti, M., Idbella, M., De Stefano, C., Mogavero, V., Allevato, E.,
811 and Bonanomi, G.: Topoclimate effect on treeline elevation depends on the regional framework: a contrast
812 between Southern Alps (New Zealand) and Apennines (Italy) forests, *Ecol. Evol.*, 13, e9733,
813 <https://doi.org/10.1002/ece3.9733>, 2023.
- 814 Rupp, T. S., Chapin, F. S., and Starfield, A. M.: Modeling the influence of topographic barriers on treeline advance
815 at the forest-tundra ecotone in northwestern Alaska, *Climatic Change*, 48, 399–416,
816 <https://doi.org/10.1023/A:1010738502596>, 2001.
- 817 Schickhoff, U., Bobrowski, M., Böhner, J., Bürzle, B., Chaudhary, R. P., Gerlitz, L., Heyken, H., Lange, J., Müller,
818 M., Scholten, T., Schwab, N., and Wedegärtner, R.: Do Himalayan treelines respond to recent climate change?



- 819 An evaluation of sensitivity indicators, *Earth Syst. Dynam.*, 6, 245–265, <https://doi.org/10.5194/esd-6-245-2015>,
820 2015.
- 821 Shi, H., Zhou, Q., He, R., Zhang, Q., and Dang, H.: Climate warming will widen the lagging gap of global treeline
822 shift relative to densification, *Agr. Forest Meteorol.*, 318, 108917,
823 <https://doi.org/10.1016/j.agrformet.2022.108917>, 2022.
- 824 Sigdel, S. R., Zheng, X., Babst, F., Camarero, J. J., Gao, S., Li, X., Lu, X., Pandey, J., Dawadi, B., Sun, J., Zhu,
825 H., Wang, T., Liang, E., and Peñuelas, J.: Accelerated succession in Himalayan alpine treelines under climatic
826 warming, *Nat. Plants*, 10, 1909–1918, <https://doi.org/10.1038/s41477-024-01855-0>, 2024.
- 827 Tian, L., Fu, W., Tao, Y., Li, M., and Wang, L.: Dynamics of the alpine timberline and its response to climate
828 change in the Hengduan mountains over the period 1985–2015, *Ecol. Indic.*, 135, 108589,
829 <https://doi.org/10.1016/j.ecolind.2022.108589>, 2022.
- 830 Treml, V. and Chuman, T.: Ecotonal dynamics of the altitudinal forest limit are affected by terrain and vegetation
831 structure variables: an example from the Sudetes Mountains in Central Europe, *Arct. Antarct. Alp. Res.*, 47, 663–
832 681, <https://doi.org/10.1657/AAAR0013-108>, 2015.
- 833 Vintsek, L., Klichowska, E., Nowak, A., and Nobis, M.: Genetic differentiation, demographic history and
834 distribution models of high alpine endemic vicariants outline the response of species to predicted climate changes
835 in a Central Asian biodiversity hotspot, *Ecol. Indic.*, 144, 109419, <https://doi.org/10.1016/j.ecolind.2022.109419>,
836 2022.
- 837 Vitali, A., Camarero, J. J., Garbarino, M., Piermattei, A., and Urbinati, C.: Deconstructing human-shaped treelines:
838 Microsite topography and distance to seed source control *Pinus nigra* colonization of treeless areas in the Italian
839 Apennines, *Forest Ecol. Manage.*, 406, 37–45, <https://doi.org/10.1016/j.foreco.2017.10.004>, 2017.
- 840 Wang, X., Wang, T., Xu, J., Shen, Z., Yang, Y., Chen, A., Wang, S., Liang, E., and Piao, S.: Enhanced habitat
841 loss of the Himalayan endemic flora driven by warming-forced upslope tree expansion, *Nat. Ecol. Evol.*, 6, 890–
842 899, <https://doi.org/10.1038/s41559-022-01774-3>, 2022.
- 843 Wang, Y., Sylvester, S. P., Lu, X., Dawadi, B., Sigdel, S. R., Liang, E., and Camarero, J. J.: The stability of spruce
844 treelines on the eastern Tibetan Plateau over the last century is explained by pastoral disturbance, *Forest Ecol.
845 Manage.*, 442, 34–45, <https://doi.org/10.1016/j.foreco.2019.03.058>, 2019.
- 846 Weckworth, B. V., Musiani, M., DeCesare, N. J., McDevitt, A. D., Hebblewhite, M., and Mariani, S.: Preferred
847 habitat and effective population size drive landscape genetic patterns in an endangered species, *P. Roy. Soc. B-
848 Biol. Sci.*, 280, 20131756, <https://doi.org/10.1098/rspb.2013.1756>, 2013.
- 849 Wei, X., Meng, H., and Jiang, M.: Landscape genetic structure of a streamside tree species *Euptelea pleiospermum*
850 (*Eupteleaceae*): Contrasting roles of river valley and mountain ridge, *PLOS ONE*, 8, e66928,
851 <https://doi.org/10.1371/journal.pone.0066928>, 2013.
- 852 Wickham, H.: *ggplot2: Elegant Graphics for Data Analysis*, Springer-Verlag, New York,
853 <https://ggplot2.tidyverse.org>, 2016.
- 854 Wieners, K.-H., Giorgetta, M., Jungclaus, J., Reick, C., Esch, M., Bittner, M., Legutke, S., Schupfner, M.,
855 Wachsmann, F., Gayler, V., Haak, H., de Vrese, P., Raddatz, T., Mauritsen, T., von Storch, J.-S., Behrens, J.,
856 Brovkin, V., Claussen, M., Crueger, T., Fast, I., Fiedler, S., Hagemann, S., Hohenegger, C., Jahns, T., Kloster, S.,
857 Kinne, S., Lasslop, G., Kornblueh, L., Marotzke, J., Matei, D., Mikolajewicz, U., Modali, K., Müller, W., Nabel,
858 J., Notz, D., Peters-von Gehlen, K., Pincus, R., Pohlmann, H., Pongratz, J., Rast, S., Schmidt, H., Schnur, R.,
859 Schulzweida, U., Six, K., Stevens, B., Voigt, A., and Roeckner, E.: MPI-M MPI-ESM1.2-LR model output



- 860 prepared for CMIP6 CMIP esm-hist, Earth System Grid Federation, <https://doi.org/10.22033/ESGF/CMIP6.6545>,
861 2019.
- 862 Wohl, E.: Connectivity in rivers, *Prog. Phys. Geogr.*, 41, 345–362, <https://doi.org/10.1177/0309133317714972>,
863 2017.
- 864 Xing, Y. W. and Ree, R. H.: Uplift-driven diversification in the Hengduan Mountains, a temperate biodiversity
865 hotspot, *P. Natl. Acad. Sci. USA*, 114, E3444–E3451, <https://doi.org/10.1073/pnas.1616063114>, 2017.
- 866 Xu, J., Wang, T., Wang, X., Körner, C., Cao, X., Liang, E., Yang, Y., and Piao, S.: Late Quaternary fluctuation
867 in upper range limit of trees shapes endemic flora diversity on the Tibetan Plateau, *Nat. Commun.*, 16, 1819,
868 <https://doi.org/10.1038/s41467-025-57036-w>, 2025.
- 869 Yan, J., Zhang, Y., Bai, W., Liu, Y., Bao, W., Liu, L., and Zheng, D.: Land cover changes based on plant
870 successions: Deforestation, rehabilitation and degeneration of forest in the upper Dadu River watershed, *Sci.*
871 *China Ser. D*, 48, 2214–2230, <https://doi.org/10.1360/04yd0128>, 2005.
- 872 Zhang, X., Ci, X., Hu, J., Bai, Y., Thornhill, A. H., Conran, J. G., and Li, J.: Riparian areas as a conservation
873 priority under climate change, *Sci. Total Environ.*, 858, 159879, <https://doi.org/10.1016/j.scitotenv.2022.159879>,
874 2023.
- 875 Zheng, L., Shi, P., Zhou, T., Hou, G., Song, M., and Yu, F.: Tree regeneration patterns on contrasting slopes at
876 treeline ecotones in eastern Tibet, *Forests*, 12, 1605, <https://doi.org/10.3390/f12111605>, 2021.
- 877 Zheng, X., Babst, F., Camarero, J. J., Li, X., Lu, X., Gao, S., Sigdel, S. R., Wang, Y., Zhu, H., and Liang, E.:
878 Density-dependent species interactions modulate alpine treeline shifts, *Ecol. Lett.*, 27, e14403,
879 <https://doi.org/10.1111/ele.14403>, 2024.
- 880 Zou, F., Tu, C., Liu, D., Yang, C., Wang, W., and Zhang, Z.: Alpine treeline dynamics and the special exposure
881 effect in the Hengduan Mountains, *Front. Plant Sci.*, 13, 861231, <https://doi.org/10.3389/fpls.2022.861231>, 2022.